Available online at www.sciencedirect.com
SCIENCE DIRECT®
International Journal of Heat and Mass Transfer 47 (2004) 5021–5031
International Journal of HEAT and MASS TRANSFER
www.elsevier.com/locate/ijhmt

Impinging premixed butane/air circular laminar flame jet—influence of impingement plate on heat transfer characteristics

Z. Zhao, T.T. Wong, C.W. Leung *

Department of Mechanical Engineering, The Hong Kong Polytechnic University, Hung Hom, Kowloon, Hong Kong

Received 26 December 2003; received in revised form 22 June 2004
Available online 23 August 2004

Abstract

Experimental studies were performed to study the heat transfer characteristics of an impingement flame jet system consisting of a premixed butane/air circular flame jet impinging vertically upward upon a horizontal rectangular plate at laminar flow condition. There were two impingement plates manufactured with brass and stainless steel respectively used in the present study. The integrated effects of Reynolds number and equivalence ratio of the air/fuel jet, and distance between the nozzle and the plate (i.e. nozzle-to-plate distance) on heat transfer characteristics of the flame jet system had been investigated. The influence in using impingement plate with different thermal conductivities, surface emissivities and roughnesses on heat flux received by the plate was examined via comparison, which had not been reported in previous literatures. A higher resistance to heat transfer had been encountered when the stainless steel impingement plate of lower thermal conductivity was used, which led to a significantly lower heat flux at the stagnation region. However, the heat flux distribution in the wall-jet region of the plate was only slightly affected by using different impingement plates. Because of the significantly lower heat transfer, more fuel was not required to consume and existed at the stagnation region of the stainless steel impingement plate, which would be burned latter in the wall-jet region to release its chemical energy and enhance the local heat flux there.

Keywords: Premixed butane/air combustion; Impingement heat transfer characteristics; Circular laminar flame jet; Influence of impingement plate

1. Introduction

Jet impingement heat transfer has been well established as a high-performance technique for heating, cooling and drying processes due to its very high heat and mass transfer. The high heat transfer associated with impinging isothermal gaseous jets has been well recognized and investigated for several years [1–8]. Compared to the considerable amount of investigations on gaseous jets, relatively few studies have been performed on the impinging flame jets, even though they are already widely applied for many industrial and domestic purposes [9–12]. The rarely availability of reports on the studies concerning with heat transfer characteristics of the impinging flame jets in the literatures may be due to their complexity, which may involve convection, conduction, radiation and thermo-chemical heat release (TCHR).

* Corresponding author. Tel.: +852 2766 6651; fax: +852 2365 4703.
E-mail address: mmcwl@polyu.edu.hk (C.W. Leung).

0017-9310/$ - see front matter © 2004 Elsevier Ltd. All rights reserved.
doi:10.1016/j.ijheatmasstransfer.2004.06.022

Nomenclature

d	diameter of the circular nozzle (m)
H	distance between the nozzle and the impingement plate (m)
A/F	air/fuel ratio
M	molecular weight (kg/kmol)
Re	Reynolds number
r	radial distance from stagnation point (m)
T	temperature (K)
Y	molar fraction

Greek symbols

μ	dynamic viscosity (m^2/s)
ρ	density (kg/m^3)
ϕ	equivalence ratio

Subscripts

exit	at the exit position
i	mixture component including fuel and gas
mix	air/fuel mixture
stoic	stoichiometric state

Most of the previous studies on impingement flame jet had been concentrated on circular jet utilizing methane or natural gas [13–18]. Baukal and Gebhart [19] found that the heating process of premixed impingement flame jet usually comprised multiple heat transfer mechanisms. In their study, polished, untreated and blackened surfaces were used to investigate the effect of surface emissivity. Conclusion was then made that both non-luminous radiation and thermo-chemical heat release were only small fraction of the total heat flux. With the use of enhanced-oxygen/natural-gas flame impinging normal to a plate [20], thermal efficiency of the system decreased with the firing rate. The heat flux was increased by 54–230% when oxygen content in the oxidizer was increasing from the normal condition of 0.21–0.30 and then to 1.00. Besides, the peak heat flux occurred at the different positions on the impingement plate.

According to the studies of Dong et al. [21–23], the premixed butane/air laminar flame jet impingement heat transfer was dependent on Reynolds number and equivalence ratio of the air/fuel jet, and configurations of the air/fuel nozzle and the impingement plate. Effects of nozzle shape (i.e. circular or slot) and inclination of the impingement plate on heat transfer characteristics of the system had been studied. The slot flame jet was found to produce more uniform and higher average heat flux than the circular flame jet. A significant amount of unburned fuel existed at the stagnation region of the impingement plate when the nozzle-to-plate distance was too small (i.e. $H/d < 2$), which shifted the location of maximum heat flux away from the stagnation point. In a similar study, Kwok et al. [24] suggested the importance in matching the flame length with the nozzle-to-plate distance to achieve the best heat transfer performance.

Most of the previous investigations about impingement flame jet system were conducted with impingement plate of excellent thermal conductivity, such as copper, brass and aluminum. Investigation conducted with impingement surface of relatively low thermal conductivity, for example steel, had only been rarely reported [25–28], even though it is already widely used in many applications. Besides, the flame type applied in investigations [25–28] was rather deviated from that of the present study, i.e. premixed flame for domestic applications. When thermal conductivity of the impingement plate is decreased, its conduction will be reduced due to the increased thermal resistance and the heat transfer characteristics of the impinging flame jet system may be significantly different. In addition, surface emissivity and roughness of the impingement surface will be affected when it is fabricated with different materials, which may also influence its radiation and convection to a certain extent.

The present experimental work was carried out to fill this gap. Influence on the heat transfer characteristics of an impinging premixed butane/air circular flame jet by changing the impingement plate was studied via comparison. There were two impingement plates fabricated with different materials, i.e. brass and stainless steel, respectively, for the present study. The two horizontally placed square impingement plates had the same shape and size, but different thermal conductivities, surface emissivities and roughnesses. Experiments were performed at a wide range of Reynolds number and equivalence ratio of the air/fuel jet, and various nozzle-to-plate distances.

2. Experimental setup and procedures

The present impingement flame jet system consisted of two parts: the heat generation system and the heat absorption system, which was shown in Fig. 1(a) In the heat generation system, a circular duct of an inner diameter of 9 mm and a length of 330 mm, was used as the nozzle (i.e. flame holder) as shown in Fig. 1(b). Metered compressed air and butane gas were premixed in a brass cylinder and then delivered to a cylindrical brass equalizing chamber via a 90 mm long stainless

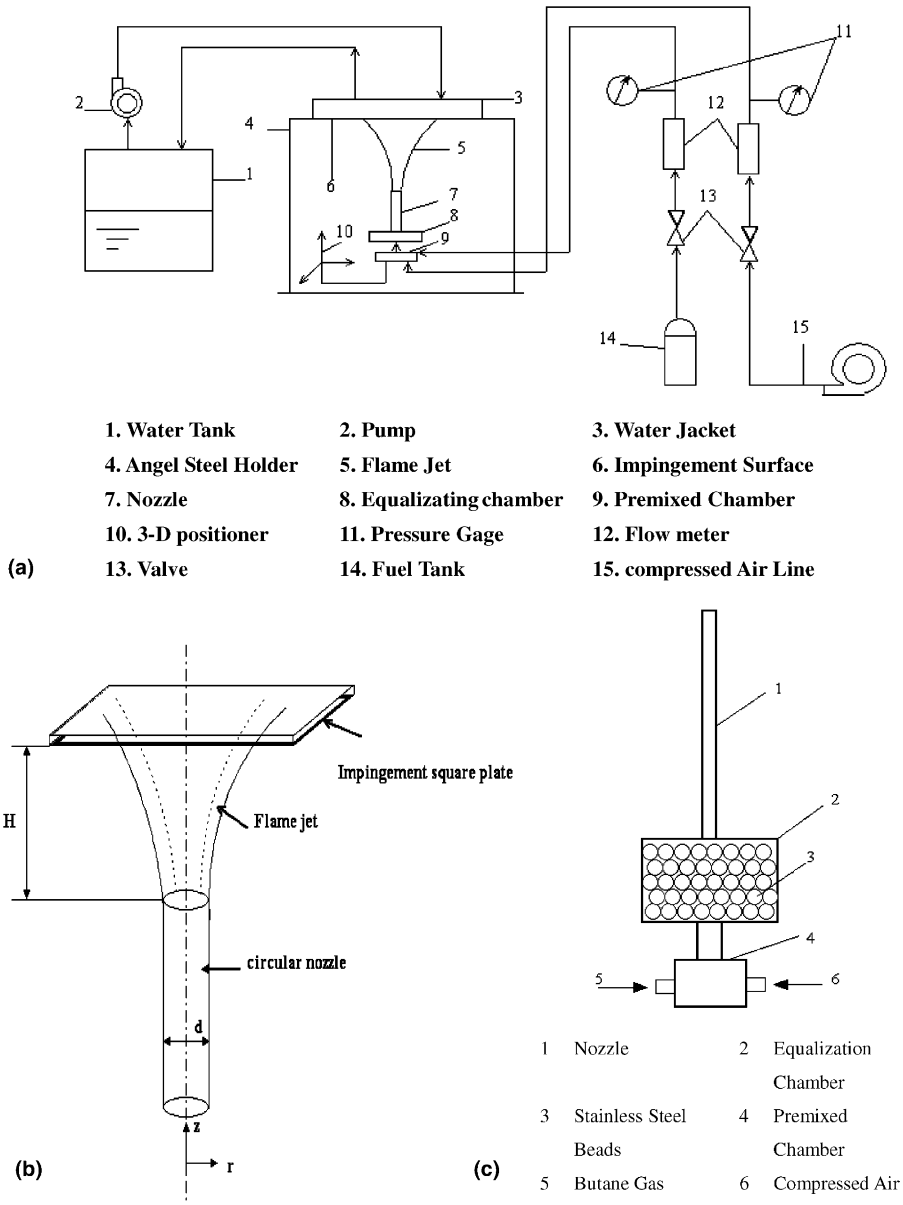

Fig. 1. (a) Schematic of the experimental setup. (b) Coordinate system. (c) Sketch of the burner of the impingement flame jet system.

steel tube. The equalization chamber, as shown in Fig. 1(c), was fully filled with very small stainless steel beads to ensure a uniform flow and avoid flashing back of the flame. The air/fuel mixture was then supplied to and ignited at the rim of the flame holder by a portable torch. Inner surface of the flame holder had been polished to facilitate a more uniform exit velocity profile. The premixed chamber, stainless steel tube, equalization chamber and circular nozzle were assembled and fixed on a three-dimensional positioner so that the flame could be moved to any desired position relative to the impingement surface.

For the present heat absorption system, there were two horizontal square impingement plates of 400 mm × 400 mm × 5 mm fabricated with brass and stainless steel, respectively. Nominal value of the thermal conductivity was obtained from Ref. [29]. Surface emissivity was recorded with a Minolta spot infrared thermometer (model: 505) with an accuracy of ±2%. The thermometer gave the surface emissivity when the recorded temperature was equal to that measured by a T-type thermocouple at the same location and time. Surface roughness was measured experimentally with an accuracy of ±2% using the method suggested by

Thomas [30]. The properties of the two plates were measured to be:

Materials	Brass	Stainless steel
Thermal conductivity (W/mK)	111.0	15.0
Surface emissivity	0.38	0.55
Surface roughness (μm)	1.035	5.188

The back of the impingement surface was uniformly cooled by a water jacket, whose top was covered by a transparent plastic plate to facilitate visualization. A thermally insulated water tank with a cross-section of 550 mm × 550 mm and a height of 650 mm was used to supply the cooling water at a constant temperature of 35 °C to the water jacket via a water pump. There were two T-type thermocouples installed to measure the inlet and outlet temperatures of the water jacket. The total heat transfer from the flame jet to the impingement plate could be determined by measuring the cooling water's flow rate and its temperature rise by passing through the water jacket. In order to achieve repeatability, measurements were only made under steady condition.

The local heat flux on the impingement surface was measured by a ceramic heat flux transducer of 4 mm × 4 mm × 0.8 mm in size with an accuracy of ±3% according to the pre-delivery calibration performed by the manufacturer, which was attached at the centre of the flame-side of the plate. The heat flux sensor was fitted into a small recess of the plate so that it was flush with the plate surface. Together with its very small dimension, installation of the heat flux sensor should provide rather negligible influence on the flow. The radial heat flux distribution on the impingement plate was measured by moving the 3-D positioner horizontally in the r-direction as shown in Fig. 1(b). The flame-side surface temperatures of the impingement plate were measured via a thermo-junction, which was located at a distance of 30 mm from the centre of the heat flux transducer. At the thermo-junction, a T-type thermocouple was embedded in a small and non-through hole, which was drilled from the rear of the impinging plate, and the joint head of the thermocouple was at a 1 mm distance from the flame-side of the plate. Due to the use of a circular nozzle and a metal impingement plate whose properties were isotropic, the surface temperatures and flame temperatures were measured along one radial direction only because of the assumption of axisymmetry. Flame temperatures were measured in the flame, right below the location of the thermo-junction, with a portable B-type thermoprobe whenever necessary. The maximum flame temperature at this spot was found to be 1400 K, which was only used to support the assumption of negligible radiation.

Experiments were conducted to compare the heat transfer characteristics of the two different impingement plates impinged by a premixed butane/air circular laminar flame jet operating at the same condition. Tests were first performed at six different jet Reynolds numbers (Re) of 500, 800, 1000, 1200, 1500, 1800 at a constant equivalence ratio (ϕ) of unity and a constant nozzle-to-plate distance (H/d) of 5. The influence of equivalence ratio was then investigated with its value fixed at 0.9, 1.0, 1.1 and 1.2 at a constant Re of 1000 and a constant H/d of 5. The influence of nozzle-to-plate distance was then investigated with the H/d ratio fixing at 3, 4, 5, 6 and 7 at a constant Re of 1000 and a constant ϕ of unity. In addition, flame shapes at different experimental conditions were recorded with a digital camera.

3. Analyses of experimental data and errors

The coordinate system used in the present study was shown in Fig. 1(b). The total heat flux received by the impingement plate was recorded with the heat flux transducer. According to Baukal and Gebhart [19], non-luminous radiation was negligible when compared to convection, which was the situation applied to the present study. On the one hand, the richest equivalence ratio adopted in the present investigation was only 1.2, and on the other hand, the maximum flame temperature was just around 1400 K. Under such experimental conditions, the assumption of non-luminous radiation was found valid according to previous investigations [21–24]. In fact, there was no soot deposition found on the flame-side surface of the impingement plate after conducting a series of experimental studies. Besides, surface emissivity of the brass plate was rather similar to that of the stainless steel plate therefore radiation was assumed to be negligible in the present work. In addition, both impingement plate surfaces had very small roughness and they were considered as very smooth. The effect of roughness on the convection could therefore be assumed negligible as suggested by Kang et al. [31].

The flame jet's Reynolds number was evaluated based on the air/fuel mixture as:

$$Re = \frac{\mu_{\text{exit}} d \rho_{\text{mix}}}{\mu_{\text{mix}}} \tag{1}$$

where μ_{mix} was calculated according to Ikoku [32] as:

$$\mu_{\text{mix}} = \frac{\sum(\mu_i Y_i \sqrt{M_i})}{\sum(Y_i \sqrt{M_i})} \tag{2}$$

The equivalence ratio, ϕ, is commonly used to indicate quantitatively the mixture strength of a fuel-oxidizer mixture (i.e. fuel-rich, fuel-lean, or stoichiometric), and is defined as:

$$\phi = \frac{(A/F)}{(A/F)_{\text{stoic}}} \tag{3}$$

Three individual tests were conducted at every prefixed operation condition. The three sets of data recorded were then averaged to ensure the repeatability and reliability of the presented experimental results. An uncertainty analysis had been carried out with the method proposed by Kline and McClintock [33]. The maximum and minimum uncertainties in surface temperature measurement were 6.1% and 1.9%, whereas those for the heat flux measurement were 7.6% and 2.9%.

4. Experimental results and discussions

Local heat flux received by the two different impingement plates from the pre-mixed butane/air circular flame jet, which was operating with the same experimental condition, were obtained. Influence of using different impingement plates on the heat transfer characteristics of the impinging flame jet system under various Reynolds numbers and equivalence ratios of the air/fuel jet, and nozzle-to-plate distances, were discussed in detail.

4.1. Influence of impingement plate under various Reynolds numbers

The Reynolds numbers (*Re*) selected were 500, 800, 1000, 1200, 1500 and 1800 to ensure a laminar flow condition, whereas the equivalence ratio (ϕ) = 1 and the nozzle-to-plate distance (*H*/*d*) = 5. All the flames under investigation presented a rather complete luminous inner reaction cone as shown in Fig. 2, whose length increased with *Re* as suggested by Dong et al. [21] and Kwok et al. [24]. There was no significant difference observed from the flame shape by changing the brass plate to stainless steel plate.

The local heat flux distribution along the radial direction of the impingement plate starting from the stagnation point was shown in Fig. 3. The variation of maximum local heat flux with *Re* was shown in Fig. 4. In general, the heat transfer performance was enhanced with *Re* for both impingement plates. According to Kwok et al. [24], length of the luminous inner reaction zone would be increased by increasing *Re* or ϕ, therefore the hottest inner reaction zone of the flame became closer to the impingement surface when *H*/*d* was kept constant. The same relationship between inner reaction zone length of the flame and *Re* was observed in the present study as shown in Fig. 2. As suggested by Hargrave et al. [17], a maximum heat flux would be occurred close to the flame's inner reaction zone because of the large concentration of reactive species there, which enhanced the convective heat transfer by their diffusion and exothermic recombination on the impingement surface. The heat transfer characteristics of the impinging flame jet system were therefore enhanced with the increasing *Re*.

It was also observed that location of the maximum heat flux was not occurred at the stagnation point of the impingement plate but shifted outwards at some distance along its radial direction. Such outward shifting of the location of maximum heat flux was increased with *Re* and became more significant for the stainless steel plate. According to Dong et al. [21], a relatively cool zone consisting of unburned fuel occurred at stagnation region of the impingement plate when the combustion was not complete at the tip of the luminous inner reaction zone, which led to a suppression of local heat flux at the stagnation point. Chemical energy obtained from further combustion of this unburned fuel at some radial distance beyond the stagnation point would result in a maximum local heat flux there. As the length of the luminous inner reaction zone was increased with *Re*, less space was available for the combustion to become fully complete, which led to the existence of a larger amount of unburned fuel at the stagnation region to enhance this shifting.

The local surface temperature distribution along the radial direction of the impingement plate starting from the stagnation point was shown in Fig. 5. There were two main points observed from Fig. 5. First, an outward shift of the maximum temperature was clearly observed, especially for the stainless steel plate. Such observation supplemented the existence of a relatively cool zone caused by the unburned fuel around the stagnation region, in particular for the stainless steel plate of lower thermal conductivity. Second, the lower thermal conductivity of the stainless steel plate had led to a relatively poor conduction and consequently a higher plate temperature.

The maximum local heat flux was lowered significantly from 310 to 165 kW/m^2 (i.e. a reduction of 88%) at *Re* = 1800, when the brass plate was replacing by the stainless steel plate due to the lower thermal conductivity and hence the higher thermal resistance encountered. Calorific value of the butane gaseous fuel could be assumed to be rather constant and therefore less fuel was consumed to produce the lower heat transfer, and more unburned fuel was then obtained at the tip of the luminous inner reaction zone. Such phenomenon led to a more significant suppression of local heat flux at the stagnation point of the stainless steel impingement plate. As more unburned fuel was consumed progressively beyond the stagnation region, location of the maximum heat flux would be shifted further away from the stagnation point.

As shown from Fig. 3, the difference in local heat flux at the wall-jet region was rather small between the brass and stainless steel impingement plates. The wall-jet

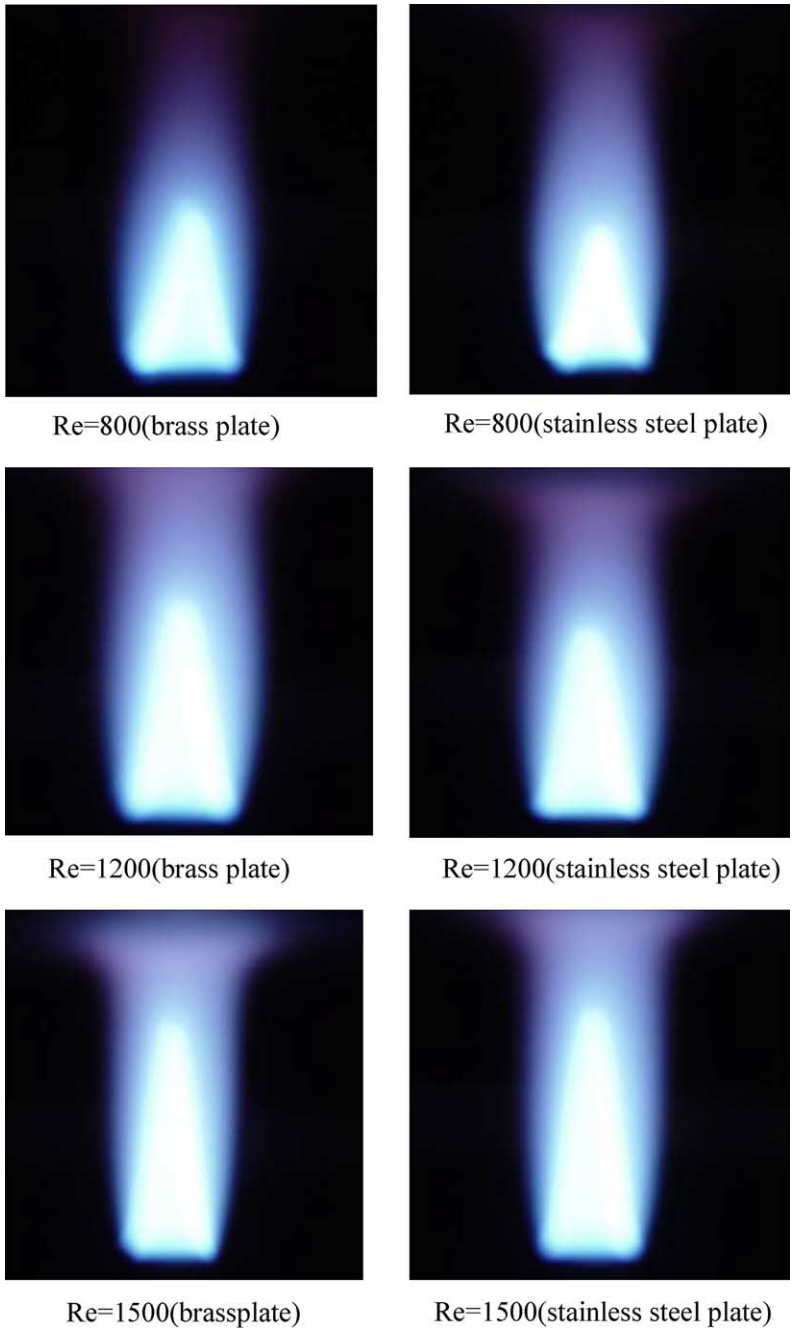

Fig. 2. Flame shapes under different Reynolds numbers ($H/d = 5$, $\phi = 1.0$).

region was identified as the region within ($0 \leqslant r/d \leqslant 5$), and the local heat flux would decrease to an almost constant and very low value away from this region. The same method had been applied in previous studies [21–24].

The minimum local heat flux received by the brass plate at $Re = 1800$ was 30 kW/m^2, but was 25 kW/m^2 for the stainless steel plate and the reduction was only 20%. The progressive combustion of more unburned fuel in the wall-jet region provided a positive effect to en-

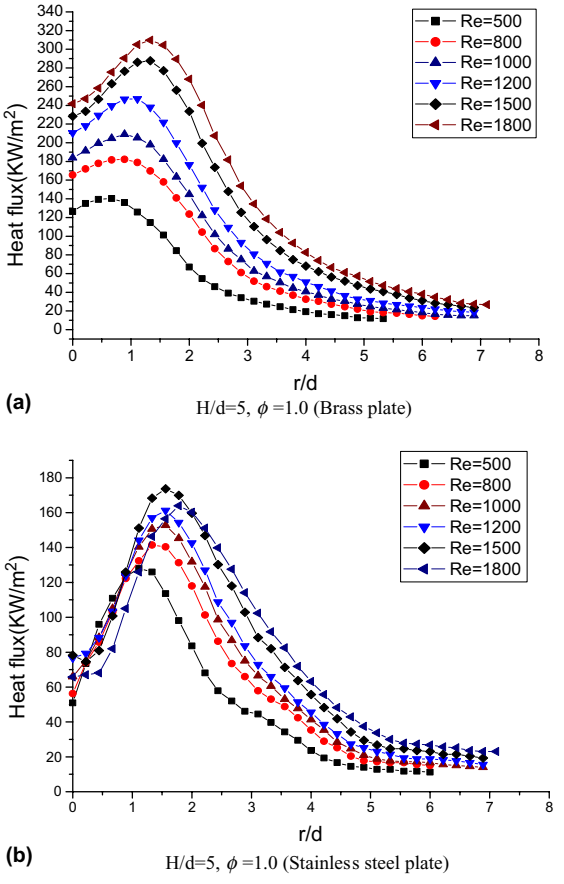

Fig. 3. Local heat flux distribution on impingement plate under different Reynolds numbers.

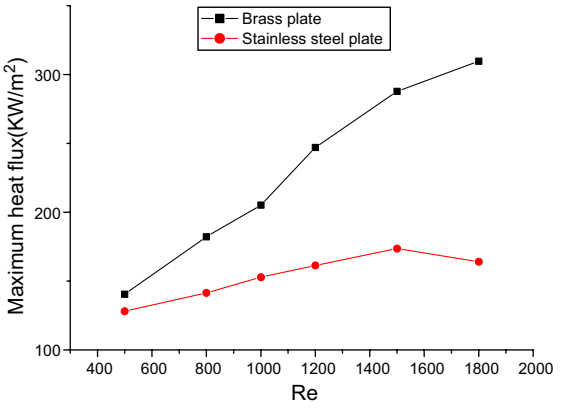

Fig. 4. Effect of *Re* on maximum heat flux (*H*/*d* = 5, ϕ = 1).

hance the heat transfer characteristics of the stainless steel impingement plate, which had compensated the adverse effect due to its lower thermal conductivity to a certain extent.

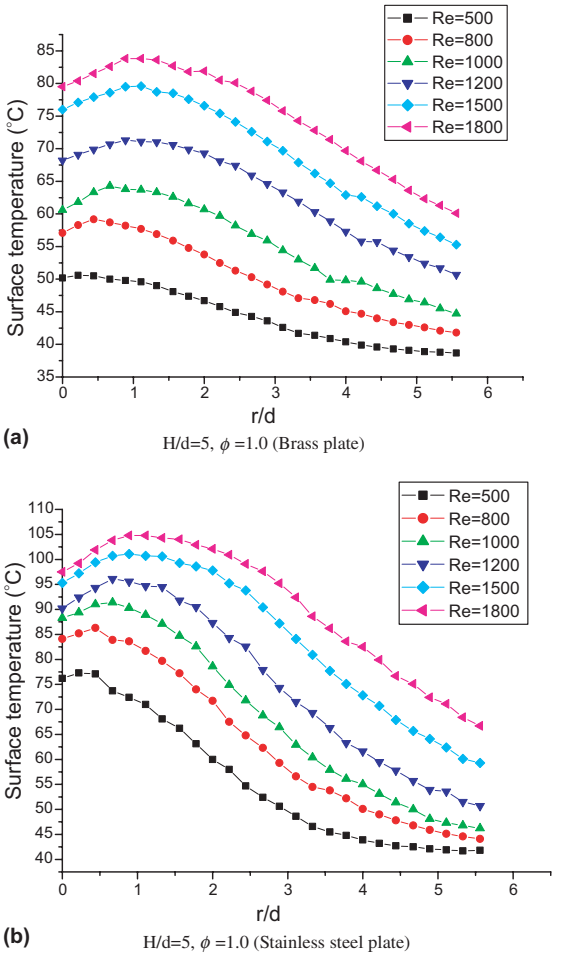

Fig. 5. Local surface temperature distribution on impingement plate under different Reynolds numbers.

A small exception was obtained with the stainless steel impingement plate, it was observed from Fig. 3 that the maximum heat flux at *Re* = 1500 was slightly higher than that at *Re* = 1800 around the stagnation region, which seemed not inline with the general trend. It should be noted that the length of the luminous inner reaction zone would increase with *Re*, and the spacing available for combustion of the flame to become complete was then reduced when the nozzle-to-plate distance was maintained unchanged. Together with the larger amount of unburned fuel at the stagnation region of the stainless steel impingement plate, the relatively cool zone at the tip of the luminous inner reaction zone was enhanced to give a larger suppression on the local heat transfer at the stagnation point of the plate. However, with the further combustion of the larger amount of unburned fuel beyond the stagnation point, heat flux at the wall-jet region became higher at *Re* = 1800.

4.2. Influence of impingement plate under various equivalence ratios

The local heat flux distributions on the two impingement plates in the radial direction starting from the stagnation point with ϕ keeping at 0.9, 1.0, 1.1 and 1.2, respectively, were shown in Fig. 6 at $Re = 1000$ and $H/d = 5$. The equivalence ratios were selected to cover the fuel-lean, stoichiometric and fuel-rich flames. In general, the heat flux received by the impingement plate was enhanced rather monotonically when ϕ was increased from 0.9 to 1.2 because of the same reason as explained in Section 4.1. However, effect of changing ϕ from 0.9 to 1.2 to enhance the shifting of the location of maximum heat flux from the stagnation point of the impingement plate was rather insignificant.

The situation was slightly different at the stagnation region of the stainless steel impingement plate. The heat flux received at the stagnation point of the plate was almost the same when ϕ was increased from 0.9 to 1.0 and 1.1, with the fuel-lean flame jet (i.e. $\phi = 0.9$) producing a slightly better heat transfer performance. However, a rather significant reduction of the heat flux at the stagnation point of the impingement plate occurred with the most fuel-rich flame jet (i.e. from 64 kW/m^2 at $\phi = 0.9$–39 kW/m^2 at $\phi = 1.2$ giving a reduction of 64%). It was again due to the particular heat transfer characteristics of the stainless steel impingement plate as explained previously, i.e. existence of a larger amount of unburned fuel at the tip of the luminous inner reaction zone. Use of a richer air/fuel mixture of $\phi = 1.2$ would certainly enhance the relatively cool zone at the stagnation region of the impingement plate, which led to a larger suppression of the local heat flux. It was evident from Fig. 6 that, a higher heat flux was occurred at the wall-jet region with the higher ϕ of 1.2, which was obtained from further combustion of the more unburned fuel.

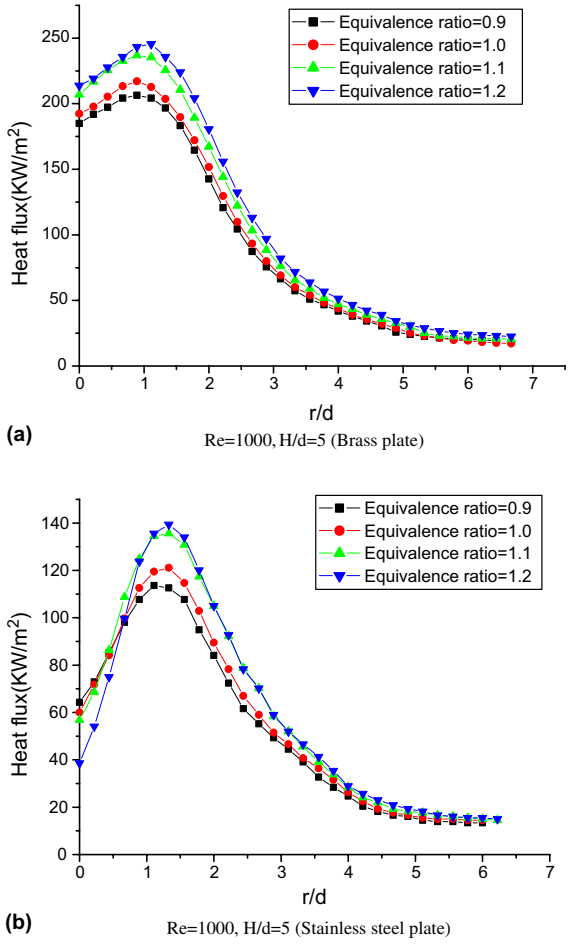

Fig. 6. Local heat flux distribution on impingement plate under different equivalence ratios.

4.3. Influence of impingement plate under various nozzle-to-plate distances

The heat flux received by the two impingement plates at different H/d ratios of 3, 4, 5, 6 and 7 were shown in Fig. 7 at $Re = 1000$ and $\phi = 1$. As observed from the flame shapes recorded by the digital camera, the luminous inner reaction zone was rather complete even when the smallest H/d ratio of 3 was used. Actually, Kwok et al. [24] suggested that the H/d ratio should be greater than 2, in order to ensure a rather complete conical shape of the luminous inner reaction zone at $Re = 1000$ and $\phi = 1$. In general, the heat flux on the plate decreased by increasing the H/d ratio in the stagnation region. However, difference between the heat transfer performances at the wall-jet region was rather insignificant when the H/d ratio was increased from 3 to 7.

For the brass impingement plate, shifting of the location of maximum heat flux from the stagnation point was almost constant for a large range of H/d ratios between 3 and 7. The heat flux received by the plate at both the stagnation region and the wall-jet region increased very slightly and linearly when the H/d ratio was decreased from 7 to 4. However, there was a significant increase of the heat flux at the stagnation region at $H/d = 3$ (i.e. 226 kW/m^2 at $H/d = 4$ whereas 273 kW/m^2 at $H/d = 3$, giving an increase of 21%). Hargrave et al. [17] suggested that a maximum heat transfer would be caused by the large concentration of reactive species existing at the tip of the flame's luminous inner reaction zone (i.e. the flame front), which enhanced the convection by their diffusion and exothermic recombination on the impingement surface. Such activities were extremely significant when the separation between the flame front and the impingement surface was not excessively

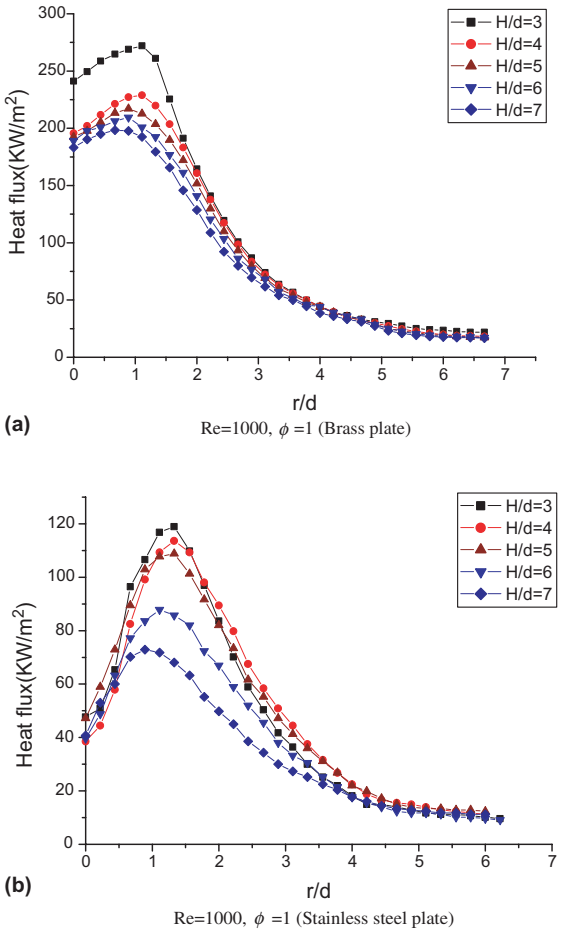

Fig. 7. Local heat flux distribution on impingement plate under different nozzle-to-plate distances.

large (i.e. at $H/d = 3$). When this separation became large enough (i.e. at $H/d > 4$), effect of such activities on the heat flux received by the impingement plate was less important.

For the stainless steel impingement plate, shifting of the location of maximum heat flux from the stagnation point slightly increased and the heat transfer performance increased slightly and linearly at the wall-jet region when the H/d ratio was reduced from 7 to 3. Concerning about the heat flux received at its stagnation region, the situation was rather different from that of the brass impingement plate. The maximum heat flux obtained at $H/d = 3$, 4 and 5 were rather similar but significantly higher than those at $H/d = 6$ and 7. This special phenomenon had been explained in the above paragraph as the diffusion and exothermic recombination of the reactive species on the impingement surface. However, due to the special heat transfer characteristics of the stainless steel impingement plate of having a larger amount of unburned fuel at the tip of the flame's luminous inner reaction zone, such activities were enhanced and maintained significant even the H/d ratio was increased from 3 to 5.

5. Conclusions

Experiments were performed to study the influence of using impingement plate of different materials (i.e. brass and stainless steel) on the heat transfer characteristics of a premixed butane/air circular laminar flame jet, which was emitting vertically upward to impinge normally on the horizontal rectangular plate. The integrated effects of Reynolds number and equivalence ratio of the butane/air jet and the nozzle-to-plate distance on heat transfer characteristics of the flame jet system had been studied. Comparisons between the heat flux received by the two impingement-plates having different thermal conductivities, surface emissivities and roughnesses, under a wide range of Re, ϕ and H/d, were made. The major conclusions of the present study could be drawn as following:

1. Thermal conductivity of the impingement plate provided the major influence on the heat transfer from the flame jet to the plate. Heat flux received by the stainless steel impingement plate was significantly lower due to the higher thermal resistance resulted from its lower thermal conductivity. The maximum local heat flux was decreased from 310 to 165 kW/m^2 at $Re = 1800$, $\phi = 1$ and $H/d = 5$, when the brass plate was replacing by the stainless steel plate. Such phenomenon was particularly notable in the stagnation region, but became less significant in the wall-jet region of the impingement plate. The minimum local heat flux received by the brass plate was 30 kW/m^2 at $Re = 1800$, $\phi = 1$ and $H/d = 5$, but was 25 kW/m^2 for the stainless steel plate at the same conditions.
2. Because of the use of very smooth surfaces for both materials, effect of surface roughness of the impingement plate on the convection between the flame jet and the plate had not been ascertained.
3. Non-luminous radiation was assumed due to the reasons as mentioned and therefore radiation was rather negligible when compared to convection. In addition, surface emissivities of the two impingement plates were quite close to each other (i.e. 0.38 and 0.55). In the present study, effect of surface emissivity of the impingement plate on the heat transfer characteristics of the impinging flame jet system had not been fully identified.
4. Use of an impingement plate of lower thermal conductivity led to a larger suppression of the heat flux at its stagnation point and enhanced the outward

shift of the location of maximum heat flux from there. Because of the lower heat transfer from the flame jet to the impingement plate of lower thermal conductivity, less fuel was only needed to consume and more unburned fuel was then obtained at the tip of the flame's luminous inner reaction zone. Existence of a larger amount of relatively cool unburned air/fuel mixture led to a more significant suppression of the local heat flux at the stagnation point of the stainless steel plate. As more unburned fuel was consumed progressively beyond the stagnation region, location of the maximum heat flux would be shifted further away from the stagnation point due to the additional chemical energy.

5. At the wall-jet region, heat transfer was essentially from the hot combustion gas to the impingement plate whereas that from the diffusion and exothermic recombination of the chemically reactive species was less significant. Therefore, a small difference was found between the heat flux received by the brass and stainless steel plates.

Acknowledgment

The authors wish to thank The Hong Kong Polytechnic University for the financial support of the present study.

References

[1] H. Martin, Heat and mass transfer between impinging gas jets and solid surfaces, Adv. Heat Transfer 13 (1977) 1–60.
[2] D.L. Button, D. Wilcox, Impingement heat transfer—A bibliography 1890–1975, Previews Heat Transfer 4 (1978) 83–98.
[3] Co. Popiel, Th. Vandermeer, Cj. Hoogendoorn, Convective heat-transfer on a plate in an impinging round hot gas-jet of low Reynolds-number, Int. J. Heat Mass Transfer 23 (8) (1980) 1055–1068.
[4] S.J. Downs, E.H. James, Jet impingement heat transfer—A literature survey, ASME Paper No. 87-H-35, ASME, New York, 1987.
[5] A.M. Huber, Heat transfer with impinging gaseous jet systems, PhD thesis, Purdue University, 1993.
[6] J.N.B. Livingood, P. Hrycak, Impinging heat transfer from turbulent air stream jets to flat plates—A literature survey, NASA TM X-2778, 1973.
[7] P. Hrycak, Heat transfer from impinging jets: A literature review, AWAL-TR-81-3054, 1981.
[8] E.M. Sparrow, T.C. Wong, Impingement transfer coefficients due to initially laminar slot jets, Int. J. Heat Mass Transfer 18 (1975) 597–605.
[9] R. Viskanta, Heat transfer to impinging isothermal gas and flame jets, Exp. Thermal Fluid Sci. 6 (1993) 111–134.
[10] C.E. Baukal, B. Gebhart, A review of flame impingement heat transfer studies. Part 1: Experimental conditions, Combust. Sci. Tech. 104 (1995) 339–357.
[11] J. Sumrerng, R. Natthawut, High efficiency heat-recirculating domestic gas burners, Exp. Thermal Fluid Sci. 26 (2002) 581–592.
[12] Pj. Ashman, R. Junus, Jf. Surbington, Gd. Sergeant, The effects of load height on the emissions from a natural gas-fired domestic cooktop burner, Combust. Sci. Technol. 103 (1–6) (1994) 283–293.
[13] C.E. Baukal, Heat transfer from lame impingement normal to a plane surface, PhD thesis, University of Pennsylvania, 1996.
[14] E. Buhr, G. Haupt, H. Kremer, Heat transfer from impinging turbulent jet flames to plane surfaces, Combust. Inst. Euro. Symp. (1973) 607–612.
[15] M. Fairweather, J.K. Kilham, S. Nawaz, Stagnation point heat transfer from laminar, high temperature methane flames, Int. J. Heat Fluid Flow 5 (1984) 225–238.
[16] G.K. Hargrave, M. Fairweather, J.K. Kilham, Forced convective heat transfer from premixed flames—Part 1: Flame structure, Int. J. Heat Fluid Flow 8 (1987) 55–63.
[17] G.K. Hargrave, M. Fairweather, J.K. Kilham, Forced convective heat transfer from premixed flames—Part 2: Impingement heat transfer, Int. J. Heat Fluid Flow 8 (1987) 132–138.
[18] A. Milson, N.A. Chigier, Studies of methane and methane–air flames impinging on a cold plate, Combust. Flame 21 (1973) 295–305.
[19] C.E. Baukal, B. Gebhart, Surface condition effect on flame impingement heat transfer, Exp. Thermal Fluid Sci. 15 (1997) 323–335.
[20] C.E. Baukal, B. Gebhart, Heat transfer from oxygen-enhanced/natural gas flames impinging normal to a plane surface, Exp. Thermal Fluid Sci. 16 (1998) 247–259.
[21] L.L. Dong, C.S. Cheung, C.W. Leung, Heat transfer characteristics of an impinging butane/air flame jet of low Reynolds number, Exp. Heat Transfer 14 (2001) 265–282.
[22] L.L. Dong, C.S. Cheung, C.W. Leung, Heat transfer from an impinging premixed butane/air slot flame jet, Int. J. Heat Mass Transfer 45 (2002) 979–992.
[23] L.L. Dong, C.W. Leung, C.S. Cheung, Heat transfer characteristics of premixed butane/air flame jets impinging on an inclined flat plate, Heat Mass Transfer 39 (2002) 19–26.
[24] L.C. Kwok, C.W. Leung, C.S. Cheung, Heat transfer characteristics of slot and round premixed impinging flame jets, Exp. Heat Transfer 16 (2003) 111–137.
[25] A. Milson, N.A. Chigier, Studies of methane and methane–air flames impinging on a cold plate, Combust. Flame 21 (1973) 295–305.
[26] R.B. Smith, T.M. Lowes, Convective heat transfer from impinging tunnel burner flames—A short report on the NG-4 trials, Int. Flame Res. Foundation, Report F 35/a/9, Netherlands, 1974.
[27] M. Matsuo, M. Hattori, T. Ohta, S. Kishimoto, The experimental results of the heat transfer by flame impingement, Int. Flame Res. Foundation, Report F 29/1a/1, Netherlands, 1978.
[28] J.B. Rajani, R. Payne, S. Michelfelder, Convective heat transfer from impinging oxygen–natural-gas flames—

Experimental results from the NG5 trials, Int. Flame Res. Foundation, Report F 35/a/12, Netherlands, 1978.
[29] A. Bejan, D.A. Kraus, Heat Transfer Handbook, Wiley & Sons, 2003.
[30] T.R. Thomas, Rough Surfaces, Imperial College Press, 1999.
[31] H.J. Kang, T.T. Wong, C.W. Leung, Effect of surface roughness on forced convection and friction in triangular ducts, Exp. Heat Transfer 11 (1998) 241–253.
[32] C.U. Ikoku, Natural Gas Production Engineering, Wiley, 1984.
[33] S.J. Kline, F.A. McClintock, Describing uncertainties in single sample experiments, Mech. Eng. 75 (1953) 3–8.